Sensors and Materials, Vol. 36, No. 8 (2024) 3433–3444
MYU Tokyo

S & M 3742

Effect of Microstructure Changes Caused by Cold Rolling on the Exothermic Characteristics of Al/Ni Multilayer Material

Souto Yamashita,[1] Hiroya Saegusa,[2] Takahiro Namazu,[2] and Shugo Miyake[3*]

[1]Department of Mechanical Engineering, Kobe City College of Technology,
8-3 Gakuenhigashi-machi, Nishi-ku, Kobe-shi, Hyogo 651-2102, Japan
[2]Faculty of Engineering, Kyoto University of Advanced Science,
18 Yamanouchi-gotanda-cho, Ukyo-ku, Kyoto 615-8577, Japan
[3]Department of Mechanical Engineering, Faculty of Science and Engineering, Setsunan University,
17-8 Ikeda-Nakamachi, Neyagawa, Osaka 572-8508, Japan

(Received May 31, 2024; accepted June 24, 2024)

Keywords: Al/Ni multilayer material, self-propagating exothermic reaction, isothermal calorimeter, standard adding method

In this study, the isothermal reaction calorimetry of an Al/Ni multilayer material fabricated by an accumulative roll bonding method was performed using an isothermal calorimeter. An additive method was also devised to measure low-reactivity materials. Calorimetry results for several different numbers of cold-rolling passes indicated that the average calorific value of the reaction improved with an increase in the number of rolling passes, and the variance decreased. The calorific value of the deposited multilayer film, which had a uniform microstructure, was also measured. A comparison of the calorific values of the reaction between the powder and films showed that, although the films had a uniform structure, the average and variance were similar. These results experimentally confirmed that, although the multilayer film is extremely reactive at Al:Ni = 1:1 atomic composition ratio, the powder and film materials are equivalent with respect to the total heat generation of the high rolling pass condition.

1. Introduction

With the widespread use of various electronic devices in our daily lives, electronic control technology has developed rapidly to address environmental issues and enhance user safety. Because electronic control devices are installed to improve product safety and convenience, packaging technology requires high reliability. However, the reflow process, which is mainly used in the current packaging technology, involves long-term heating using an electronic furnace or infrared rays. Prolonged heating during the reflow process causes the thermal fatigue of the metal components and warping of the substrate, which may result in joint failure. Furthermore, the reflow process has an environmental impact because it consumes a significant amount of electricity. Therefore, developing a new joining technology that uses a local heating source with low environmental impact is crucial. In such situations, the self-propagating exothermic reaction

*Corresponding author: e-mail: shugo.myake@setsunan.ac.jp
https://doi.org/10.18494/SAM5163

ISSN 0914-4935

between Al and Ni has attracted attention. Such a reaction is induced by a spark, producing a large amount of heat with only a small amount of material. Research has been conducted to apply Al/Ni self-propagating exothermic reactions with these characteristics to develop a new local heating technology.[1–16]

To realize a continuous and uniform self-propagating exothermic reaction of Al/Ni, fabricating a multilayer Al/Ni structure is necessary. Materials used for self-propagating exothermic reactions with an Al/Ni multilayer structure are called Al/Ni multilayer materials. Al/Ni multilayer materials have been proposed in various forms, from powders fabricated by cold rolling and pulverizing methods[5–8] to films deposited by DC magnetron sputtering.[9–16]

In this self-propagating exothermic reaction, when an Al-Ni intermetallic compound is formed, the enthalpies of formation are released as reaction heat. Differential scanning calorimetry, which uses a heater, is typically used for calorimetric measurements involving phase changes, such as the Al-Ni self-propagating exothermic reaction.[17–20] However, as previously mentioned, a key characteristic of self-propagating exothermic reactions is that they can be induced only by microsparks, having a smaller environmental impact than heater heating. Therefore, when these materials are applied to joining technology, induction by sparking is assumed instead of using a heater. Therefore, directly measuring the calorific value of multilayered materials induced by sparking is considered necessary. This approach allows for the accurate measurement of both the instantaneous phase change during the reaction and the calorific value of the reaction associated with compound formation. Therefore, in a previous study, we developed an isothermal calorimeter capable of directly measuring the calorific value of multilayer materials induced by sparking.[21] Results from experiments using that calorimeter showed an increase in calorific value with the number of rolling passes. However, multilayer powders with low-rolling passes have nonuniform multilayer structures, and some of the powders used were considered not to react uniformly. Therefore, the calorific value of multilayer powders with low-rolling passes may have been estimated to be lower than if all the powders had reacted uniformly. Further investigation of the relationship between the calorific value and the number of rolling passes requires ensuring that all the samples react uniformly and their calorific values are accurately measured, even for samples with low-rolling passes and low reactivity.

In this study, a method was devised in which a low-rolling-pass sample with low reactivity is assisted by the addition of a high-rolling-pass material with high reactivity, ensuring that all samples react uniformly and allowing for the accurate measurement of the calorific value. On the basis of the results, the relationship between the calorific value and the changes in microstructure with an increasing number of rolling passes is discussed. In addition, the effect of the uniformity of the multilayer structure on the calorific value is examined by comparing the heat of reaction of a film sample with a uniform multilayer structure to that of a powder sample fabricated by rolling.

2. Isothermal Calorimeter

We used a modified calorimeter based on an isothermal calorimeter developed in a previous study. This calorimeter features an isothermal layer made of an acrylic container filled with water, surrounded by an insulation layer made of commercially available thermal insulation material [with thermal conductivity < 0.035 W/(m•K)], as shown in Fig. 1. A vacuum insulation vessel with a double-layered insulating structure was fixed in the water tank. The calorimeters were installed in a climate-controlled laboratory, and the entire system was maintained at thermal equilibrium.

The vacuum insulation vessel inside the tank was filled with an inert liquid that was constantly stirred using a magnetic stirrer. The sample cell was made by processing a 12-μm-thick polyethylene film. During the reaction of Al/Ni multilayer powders, the polyethylene film was slightly melted by the exothermic reaction heat. Consequently, the reacted powders diffused into the inert liquid, which absorbed the reaction heat. The heat of melting of the polyethylene film used was −51.1 J/g. This film melted approximately 0.01 to 0.02 g during the reaction, converting to approximately 0.5 to 1.0 J of heat. Therefore, the measurement error due to the heat of melting of this film was evaluated to be very small and negligible. To measure the calorific value of the reaction, a thermistor (Tateyama Kagaku Kogyo, DS-103) was placed in the inert liquid, and the temperature difference was measured. The calorific value of the reaction was calculated using the temperature difference of the inert liquids.

3. Calorimetric Accuracy

3.1 Temperature stability of developed isothermal calorimeter

Figure 2 shows the temperature data of the inert liquid measured by the thermistor in the vacuum insulation vessel and the room temperature data measured by a type-K thermocouple

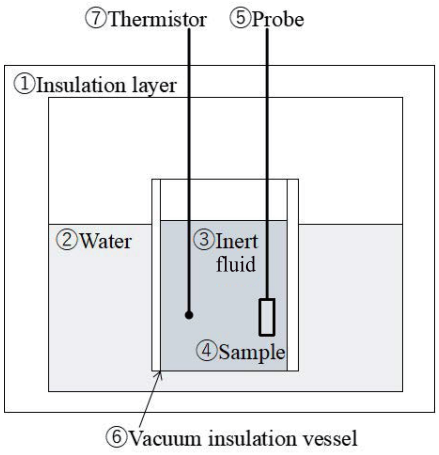

Fig. 1. (Color online) Schematic of isothermal calorimeter.

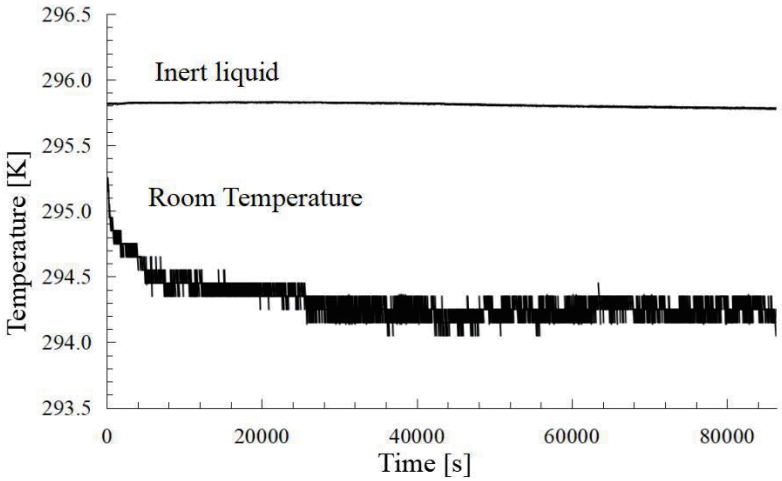

Fig. 2. Temperature stability of developed isothermal calorimeter.

placed near the calorimeter. These data were collected in an air-conditioned laboratory from the start of air conditioning. The air conditioning was set at 294.15 K. The difference between the temperature of the inert liquid and the room temperature can be attributed to individual differences in the type K thermocouple. The type K thermocouple has a temperature resolution of 0.1 K, and the room temperature changed by approximately 1 K in 24 h. In contrast, the thermistor has a temperature resolution of 0.001 K. The temperature of the inert liquid was measured every 10000 s at eight points with a standard deviation of 0.015 K. If we assume that a temperature change of ±0.015 K occurs in 86400 s (24 h), the temperature change per second is estimated to be $\pm 1.7 \times 10^{-7}$ K/s. In the measurement, it took approximately 1800 s (30 min) to be in a thermal equilibrium state with completed exothermic reaction. From this supposition, the temperature changes during measurement were estimated to be ±0.000306 K. Therefore, these changes were kept below the output resolution of the thermistor. Therefore, the heat flux between room temperature and the inert liquid was considered negligible, and this experimental system was considered to be in thermal equilibrium, well within the observable range.

3.2 Calculation method for calorific value of the reaction

In this experiment, Al/Ni multilayer powder was reacted with an inert liquid. The calorific value of the reaction was calculated from the temperature difference obtained before and after the reaction and the heat capacity of the inert liquid.

The moving average of the slope was calculated every 250 s from the start of the measurement. The slope represents the rate of temperature change per second. When the slope is less than 0.000015 K/s, which is 1/1000 of the temperature change of an inert liquid over 24 h, the liquid is considered to be in a state of sufficient thermal equilibrium. Figure 3 shows the temperature change in the inert liquid during the measurement. There was an instantaneous temperature increase near point 2, as shown in Fig. 3. This increase occurred owing to the proximity of the thermistor to the reaction sample, which was measured directly before the heat

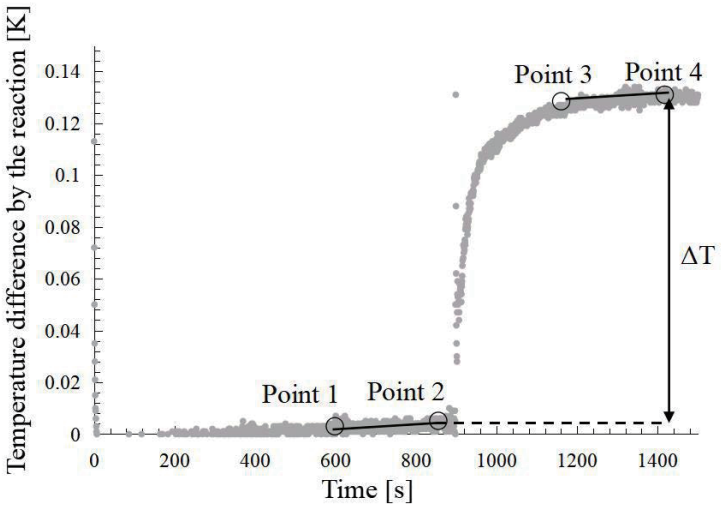

Fig. 3. Calculation of temperature difference obtained before and after reaction.

diffused into the inert liquid. In this measurement, the temperature difference in sufficient thermal equilibrium was evaluated; therefore, this noise could be ignored. The point at which the rate of temperature change exceeded 0.000015 K/s for the first time since the start of the measurement was defined as point 1 (250 s before the start of the reaction), and a regression line was plotted using the slope and intercept at that point. The point on this regression line 250 s after point 1 was then defined as point 2 (the point at which the reaction started). Next, the point that could be considered to be in sufficient thermal equilibrium for the first time after the reaction was defined as point 3. Point 4 (the point at which the reaction ended) was defined from point 3 as well as point 2. The temperature difference between points 2 and 4 was defined as the temperature difference ΔT obtained before and after the reaction.

$$q = \frac{C\Delta T}{m} \tag{1}$$

The temperature difference was multiplied by the heat capacity and divided by the mass of the sample used in the reaction to evaluate the calorific value of the reaction per gram, q, as shown in Eq. (1). In Eq. (1), C is the heat capacity of the inert liquid and m is the sample mass. In this study, C was calculated by multiplying the mass of the inert liquid used in the experiment by its specific heat.

3.3 Calorimeter measurement accuracy

The output resolution of the thermistor used in this experiment is ±0.001 K. In addition, the heat capacity of the inert liquid used in the experiment is 525 J/K for 500 g. Therefore, the error in calorimetric measurement due to the output resolution of the thermistor is approximately ±0.525 J, which is sufficiently small compared with the later described calorific value of the reaction, in the range of 1000–1600 J.

As mentioned previously, this modified calorimeter is highly accurate regarding the expected calorific value. Therefore, any variance in the calculated calorific values was considered to be solely due to the sample used in this study.

4. Effectiveness of Standard Addition Methods in Reaction Experiments

In this section, we describe the calorimetric calculation method for low-rolling-pass powders used in this study. In calorimetric measurements of powder materials using isothermal calorimetry, a powder with a low number of rolling passes tends to exhibit low reactivity. The Al/Ni multilayer powders feature a fine multilayer structure formed by the repeated rolling of alternating Al and Ni foil layers. However, as shown in Fig. 4, the low-rolling-pass powders exhibit a nonuniform multilayer structure and discontinuity in the Al/Ni reaction interface. Therefore, the low-rolling-pass powders were generally less reactive, raising uncertainty regarding the contribution of all the powders used in the reaction.

In this experiment, we assisted the reaction with a low-reactivity powder by adding 40-pass rolling powder, which has high reactivity. This attempt was to evaluate the calorific value of the low-rolling-pass powder by subtracting the calorific value of the 40-pass rolling powder after calculating the calorific value.

Figure 5 shows the diffraction peaks of the powder before the reaction, where only the Al and Ni peaks were observed. Figure 6 shows the diffraction peaks when the powder was completely reacted.

When the Al/Ni multilayer powder was fully reacted, the Al and Ni peaks disappeared regardless of the number of rolling passes, and only the peaks of Al and Ni intermetallic compounds, such as NiAl and Ni_2Al_3, were observed.

Thus, even low-rolling-pass powders can fully react through repeated sparking. However, in actual isothermal calorimetry measurements, a single spark melts the sample cell, and the powder diffuses into the inert liquid. Therefore, producing repeated sparks to fully react with all amounts of powder is not feasible. Figure 7 shows the diffraction peaks of the powders that

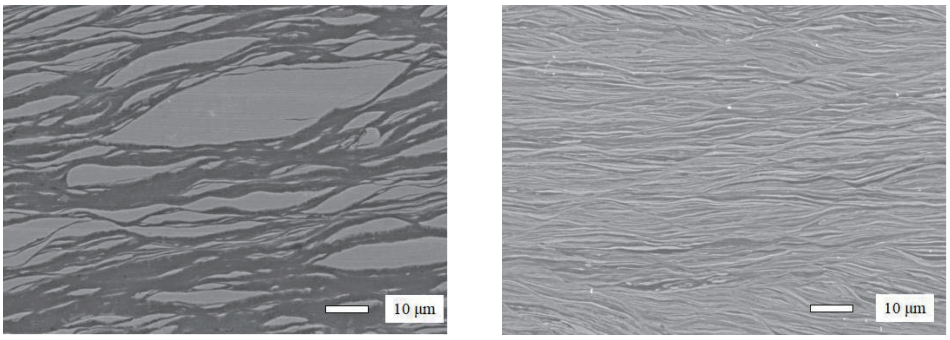

(a) (b)

Fig. 4. Cross section of Al/Ni multilayer powder material before reaction. (a) 20-pass and (b) 40-pass.

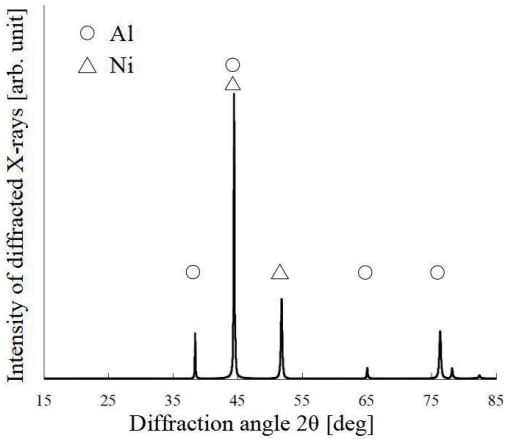

Fig. 5. Diffraction peaks of Al/Ni multilayer powder before reaction.

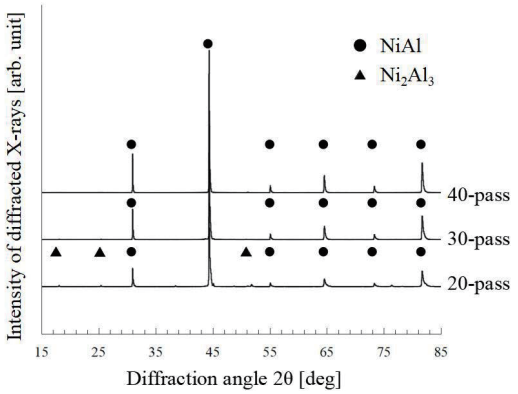

Fig. 6. Diffraction peaks of Al/Ni multilayer powder after reaction.

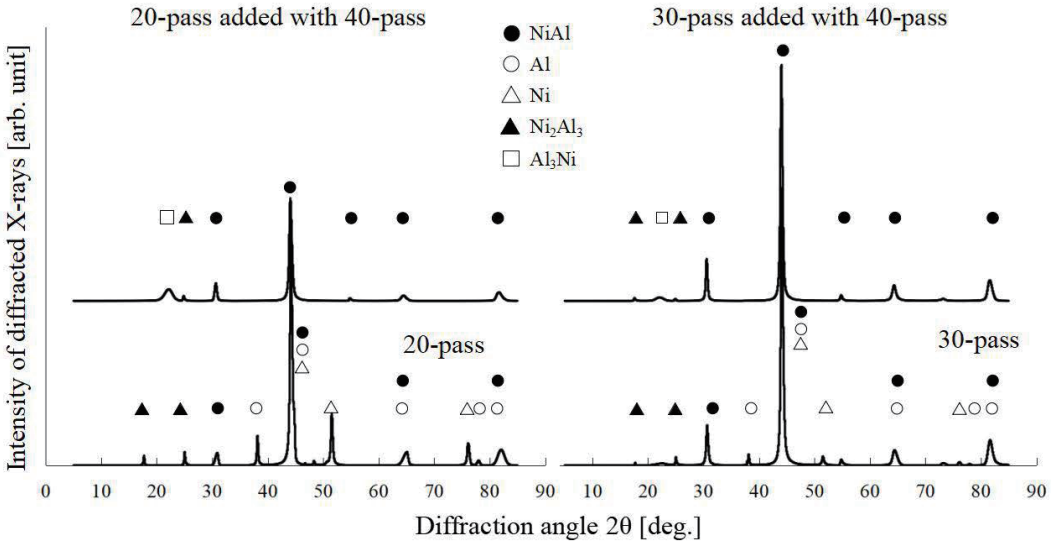

Fig. 7. Diffraction lines of low-rolling-pass powder reacted in a single spark.

reacted with a single spark. As shown in Fig. 7, the low-rolling-pass powders still exhibited peaks corresponding to Ni and Al, indicating the presence of the remaining unreacted powder.

However, as shown in Fig. 7, in the case of the sample that reacted by adding 40-pass rolling powder to the low-rolling-pass sample, the peaks of Ni and Al disappeared after the reaction, and only the peaks of intermetallic compounds such as NiAl were observed. This suggests that in this experiment, the addition of 40-pass rolling powder to the low-rolling-pass sample made it possible to react all the low-reactivity powders in a single spark. The overall calorific value of the reaction can be considered as the sum of the reaction heat of the low-rolling-pass powder and that of the 40-pass rolling powder, as shown in Eq. (2).

$$\begin{aligned} q &= \Sigma q_n \\ &= q_{20} + q_{40} \\ &= \frac{C\Delta T_{20}}{m_{20}} + \frac{C\Delta T_{40}}{m_{40}} \end{aligned} \tag{2}$$

Because the 40-pass rolling powder was highly reactive, its calorific value was measured independently and set to a known value. Next, the calorific value of the reaction between the low-rolling-pass powder and the 40-pass rolling powder was measured, and the calorific value of the 40-pass rolling powder was subtracted from the result. The resulting value was calculated as the calorific value of the low-rolling-pass powder.

5. Measurement of Calorific Value of the Reaction

5.1 Measurement of calorific value of the reaction of multilayer powder materials

The calorimetric measurements of Al/Ni multilayer powder materials using the previously mentioned method are described below. In the table, Ave. and Var. represent the average and variance in three measurements, respectively. The variance of this measurement indicates the variation in calorific value every sample.

As shown in Table 1 and Fig. 8, the average calorific value of the reaction increased with the number of rolling passes. Among the Al-Ni intermetallic compounds, NiAl boasts the highest enthalpy of formation, reportedly in the range of −60–70 J/mol.[22–26] Therefore, the calorific value per gram was estimated at 1634 J/g based on this enthalpy of formation. For the 40-pass rolling powder, the average calorific value of the reaction was found to be 1601 J/g, a value in close alignment with the estimation derived from the enthalpies of formation. Furthermore, the variance in the calorific value, calculated from repeated measurements, increased as the number of rolling passes decreased. As shown in Fig. 4, the Al/Ni reaction interface appeared discontinuous, with the layer thickness showing less uniformity in the 20-pass rolling powder than in the 40-pass rolling powder. Therefore, it is considered that the nonuniform reaction in which Al:Ni is not 1:1 occurs in the 20-pass rolling powder. As a result, it was presumed that intermetallic compounds with enthalpies of formation lower than that of NiAl, such as Ni_2Al_3

Table 1
Calorific value of the reaction for each rolling pass of multilayer powder material.

Powder (20-pass)				Powder (30-pass)				Powder (40-pass)		
m_{20} (g)	m_{40} (g)	ΔT_{20} (K)	q_{20} (J/g)	m_{30} (g)	m_{40} (g)	ΔT_{30} (K)	q_{30} (J/g)	m (g)	ΔT (K)	q (J/g)
0.026	0.013	0.043	910.3	0.022	0.009	0.055	1316.4	0.033	0.094	1656.7
0.022	0.011	0.054	1334.1	0.021	0.012	0.064	1633.8	0.033	0.094	1622.8
0.028	0.006	0.079	1537.8	0.031	0.010	0.095	1594.7	0.026	0.067	1523.4
		Ave.	1260.7			Ave.	1515.0		Ave.	1601.0
		Var.	320.1			Var.	173.0		Var.	69.3

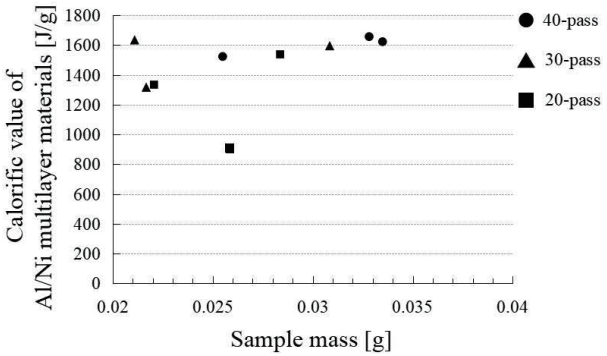

Fig. 8. Calorific value of the reaction for each rolling pass of multilayer powder material.

and Al_3Ni, were formed, reducing the overall calorific value of the reaction. However, there were instances where values close to 1600 J/g were measured for the 20- and 30-pass rolling powders. This indicates that, in some cases, the reaction is maximized in sample sets containing a high percentage of powders with atomic composition ratios close to 1:1.

5.2 Calorimetry of multilayer film materials

Next, we describe the measurement results of the Al/Ni multilayer thin films deposited via sputtering. In this experiment, the Al/Ni multilayer film had an overall thickness of 30 μm and a bilayer thickness of 100 nm.

As shown in Table 2 and Fig. 9, the average calorific value of the Al/Ni multilayer reaction is 1617 J/g, which is close to the calorific value of the 40-pass rolling powder. This value aligns closely with the calorific value calculated from the enthalpies of formation. In addition, the variances of repeated measurements for both the multilayer film and the 40-pass rolling powder were similar. This indicates that the multilayer powder and multilayer film were comparably uniform in terms of variations in calorific value. As mentioned previously, the variance in calorific value decreased as the uniformity of the Al/Ni multilayer structure improved with an increasing number of rolling passes. Here, we compare the cross sections of the multilayer film and multilayer powder.

Figure 10 shows the SEM cross sections of the multilayer thin film and multilayer powder. As shown in Fig. 10, the powder shows a multilayer structure with Al and Ni layers spaced 0.5 to 1

Table 2
Calorific values of the reaction of multilayer film and powder (40-pass rolled).

Film			Powder (40-pass)		
m (g)	ΔT (K)	q (J/g)	m (g)	ΔT (K)	q (J/g)
0.029	0.089	1616.2	0.033	0.094	1656.7
0.035	0.114	1707.6	0.033	0.094	1622.8
0.034	0.099	1527.2	0.026	0.067	1523.4
	Ave.	1617.0		Ave.	1601.0
	Var.	64.6		Var.	69.3

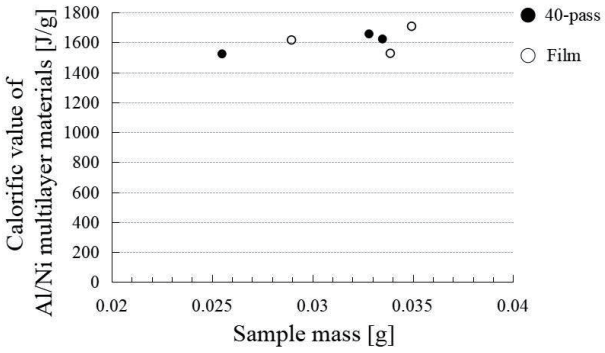

Fig. 9. Calorific values of the reaction of multilayer film and powder (40-pass rolled).

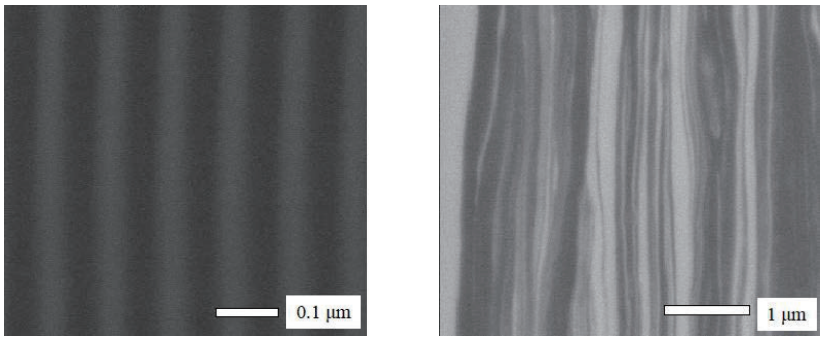

(a) (b)

Fig. 10. Cross-sectional SEM images of multilayer materials. (a) Film and (b) powder.

μm apart. In contrast, the multilayers in the film are deposited approximately 100 nm apart, which is roughly one-tenth the size of the powder material. Therefore, in terms of microstructure, multilayer films exhibit greater uniformity than multilayer powders. Furthermore, this high uniformity in the microstructure significantly affects the reaction rate.

Figure 11 shows the results of the exothermal temperature measurements for the powder and film materials using a radiation thermometer. The measurement resolution of the radiation thermometer and data logger is 100 ms. This measurement was started when the exothermic temperature reached 800 °C and was terminated when the temperature fell below 800 °C. The maximum temperatures reached by the multilayer powder and multilayer film were comparable, at approximately 1500 °C. However, the exothermic response of the multilayer film was completed in less than 300 ms, whereas the multilayer powder reached its maximum temperature in 200 ms but took an additional 1000 ms to complete the reaction. The high reaction rate of the multilayer film is presumably due to its extremely uniform microstructure and continuous reaction interface. In contrast, powders fabricated by rolling exhibit a nonuniform microstructure, resulting in a low reaction rate.

However, the previously mentioned calorific value measurement results indicate that the average and its variance are the same in both the film and the powder. Therefore, in terms of calorific value, it is considered that reducing the layer thickness of the powder to 0.5–1 μm

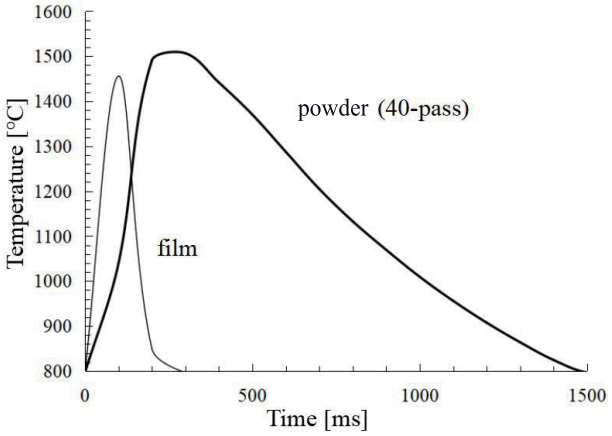

Fig. 11. Representative temperature curves of multilayer powders and films.

through rolling allows the control of the variance of the calorific value of the reaction to the same level as that of the multilayer film with a bilayer thickness of 100 nm.

6. Conclusion

In this study, a modified isothermal calorimeter was developed to measure the calorific value of the reaction from the self-propagating exothermic reaction of Al/Ni multilayer materials, and both the multilayer powder and film were measured. Adding 40-pass rolling powder, which has higher reactivity, to the weakly reactive powder enabled the reaction of all powders with a single spark. This method enabled us to evaluate the calorific value of the low-rolling-pass powder and discuss the relationship between the number of rolling passes and the calorific value.

The measurements of the powder material showed that the maximum value at each rolling pass closely matched the calorific value estimated from the formation enthalpies in which the Al:Ni ratio was 1:1. However, for the low-rolling-pass samples, a large variance in the calorific value was observed for every sample, which decreased as the number of rolling passes increased. This variance reduction can be attributed to the increased uniformity of the layer thickness in the multilayer material with more rolling passes, leading to the improved continuity of the reaction interface. Consequently, this enhancement increased the NiAl ratio in the intermetallic compound formed by the reaction, thus maximizing the calorific value of the reaction.

We then measured the calorific values of a multilayer film material with a very uniform multilayer structure fabricated using sputter deposition and 40-pass rolling powder. We found that the average calorific values and their variances were comparable. A comparison of the SEM images of the multilayer powder and film revealed that the multilayer powder was approximately 10 times thicker than the film. From these results, it is considered that reducing the layer thickness of the powder to 0.5–1 μm through rolling allows the control of the variance of the calorific value of the reaction to the same level as that of the multilayer film with a bilayer thickness of 100 nm.

Acknowledgments

We thank T. Ute and H. Ikushima (Kobe City College of Technology) for their helpful discussions and sample preparation. We also received generous support from Professor M. Takashiri (Tokai University) for the measurement of the heat of melting of the polyethylene film.

References

1 J. Wang, E. Besnoin, O. M. Knio, and T. P. Weihs: J. Appl. Phys. **95** (2004) 248. https://doi.org/10.1063/1.1629390
2 J. Wang, E. Besnoin, O. M. Knio, and T. P. Weihs: Acta Mater. **52** (2004) 5265. https://doi.org/10.1016/j.actamat.2004.07.012
3 R. Knepper, M. R. Snyder, G. Fritz, K. Fisher, O. M. Knio, and T. P. Weihs: J. Appl. Phys. **105** (2009) 083504. https://doi.org/10.1063/1.3087490
4 B. Boettge, J. Braeuer, M. Wiemer, M. Petzold, J. Bagdahn, and T. Gessner: J. Micromech. Microeng. **20** (2010) 064018. https://doi.org/10.1088/0960-1317/20/6/064018
5 S. Yamashita, R. Yamamoto, and S. Miyake: Jpn. J. Appl. Phys. **60** (2021) SCCL07. https://doi.org/10.35848/1347-4065/abe996
6 S. Miyake, T. Izumi, and R. Yamamoto: Materials **13** (2020) 4394. https://doi.org/10.3390/ma13194394
7 T. Izumi, N. Kametani, S. Miyake, S. Kanetsuki, and T. Namazu: Jpn. J. Appl. Phys. **57** (2018) 06HJ10. https://doi.org/10.7567/JJAP.57.06HJ10
8 R. Yamamoto, S. Miyake, S. Kanetsuki, T. Namazu, D. Goto, Y. Kuntani, and T. Koganezawa: J. JSEM **19** (2019) 30. https://doi.org/10.11395/jjsem.19.30
9 T. Namazu, H. Takemoto, H. Fujita, Y. Nagai and S. Inoue: Proc. 2006 IEEE 19th Micro Electromechanical Systems Conf. (IEEE, 2006) 286. https://doi.org/10.1109/MEMSYS.2006.1627792
10 T. Namazu, K. Ohtani, K. Yoshiki, and S. Inoue: Proc. 2011 16th Int. Solid-State Sensors, Actuators and Microsystems Conf. (2011) 1368. https://doi.org/10.4028/www.scientific.net/MSF.706-709.1979
11 K. Ohtani, Y. Yamano, T. Namazu, and S. Inoue: Proc. Transducers (2009) 172.
12 T. Namazu, and S. Inoue: Mater. Sci. Forum **638–642** (2010) 2142. https://doi.org/10.4028/www.scientific.net/MSF.638-642.2142
13 T. Namazu, K. Ohtani, S. Inoue, and S. Miyake: J. Eng. Mater. Technol. **137** (2015) 031011. https://doi.org/10.1115/1.4030413
14 K. Maekawa, S. Ito, and T. Namazu: Jpn. J Appl. Phys. **59** (2020) SIIL01. https://doi.org/10.35848/1347-4065/ab769b
15 S. Miyake, S. Kanetsuki, K. Morino, J. Kuroishi, and T. Namazu: Jpn. J Appl. Phys. **54** (2015) 06FP15. https://doi.org/10.7567/JJAP.54.06FP15
16 K. Maekawa, K. Kodama, S. Miyake, and T. Namazu: Jpn. J Appl. Phys. **60** (2021) SCCL15. https://doi.org/10.35848/1347-4065/abf39c
17 A. J. Gavens, D. Van Heerden, A. B. Mann, M. E. Reiss, and T. P. Weihs: J. Appl. Phys. **87** (2000) 1255. https://doi.org/10.1063/1.372005
18 H. Sina, K. B. Surredi, and S. Iyengar: J. Alloys Compd. **661** (2009) 294. https://doi.org/10.1016/j.jallcom.2015.11.105
19 A. Abraham, H. Nie, M. Schoenitz, A. B. Vorozhtsov, M. Lerner, A. Pervikov, N. Podkevich, and E. L. Dreizin: Combust. Flame **173** (2016) 179. https://doi.org/10.1016/j.combustflame.2016.08.015
20 Z. Ding, Q. Hu, W. Lu, S. Sun, M. Xia, and J. Li: Scripta Mater. **130** (2017) 214. https://doi.org/10.1016/j.scriptamat.2016.12.010
21 S. Miyake, A. Nagai, and K. Yamada: JSEM **19** (2019) 19. https://doi.org/10.11395/jjsem.19.19
22 A. S. Ramos, M. T. Vieira, J. Morgiel, J. Grzonka, S. Simoes, and M. F. Vieira: J. Alloys Compd. **484** (2009) 335. https://doi.org/10.1016/j.jallcom.2009.04.098
23 K. Rzyman, Z. Moser, R. E. Watson, and M. Weinert: J. Phase Equilibria **19** (1998) 106. https://doi.org/10.1361/105497198770342562
24 K. Rzyman and Z. Moser: Prog. Mater Sci. **49** (2004) 581. https://doi.org/10.1016/j.pmatsci.2003.08.001
25 R. Hu, P. Nash, and Q. Chen: J. Phase Equilibria Diffus. **30** (2009) 559. https://doi.org/10.1007/s11669-009-9573-3
26 F. Z. Chrifi-Alaoui, M. Nassik, K. Mahdouk, and J. C. Gachon: J. Alloys Compd. **364** (2004) 121. https://doi.org/10.1016/S0925-8388(03)00493-6